Proc. Natl. Acad. Sci. USA
Vol. 96, pp. 3228–3233, March 1999
Neurobiology

Plaque-independent disruption of neural circuits in Alzheimer's disease mouse models

ALBERT Y. HSIA*†‡, ELIEZER MASLIAH§, LISA MCCONLOGUE¶, GUI-QIU YU‖, GWEN TATSUNO¶, KANG HU¶, DORA KHOLODENKO¶, ROBERT C. MALENKA†**, ROGER A. NICOLL*†, AND LENNART MUCKE¶††‡‡

Departments of *Cellular and Molecular Pharmacology, †Physiology, **Psychiatry, and ††Neurology, University of California at San Francisco, San Francisco, CA 94143-0450; §Departments of Neurosciences and Pathology, University of California at San Diego, La Jolla, CA 92093-0624; ¶Elan Pharmaceuticals, South San Francisco, CA 94080; and ‖Gladstone Institute of Neurological Disease, San Francisco, CA 94141-9100

Contributed by Roger A. Nicoll, January 12, 1999

ABSTRACT **Autosomal dominant forms of familial Alzheimer's disease (FAD) are associated with increased production of the amyloid β peptide, Aβ42, which is derived from the amyloid protein precursor (APP). In FAD, as well as in sporadic forms of the illness, Aβ peptides accumulate abnormally in the brain in the form of amyloid plaques. Here, we show that overexpression of FAD($717_{V\rightarrow F}$)-mutant human APP in neurons of transgenic mice decreases the density of presynaptic terminals and neurons well before these mice develop amyloid plaques. Electrophysiological recordings from the hippocampus revealed prominent deficits in synaptic transmission, which also preceded amyloid deposition by several months. Although in young mice, functional and structural neuronal deficits were of similar magnitude, functional deficits became predominant with advancing age. Increased Aβ production in the context of decreased overall APP expression, achieved by addition of the Swedish FAD mutation to the APP transgene in a second line of mice, further increased synaptic transmission deficits in young APP mice without plaques. These results suggest a neurotoxic effect of Aβ that is independent of plaque formation.**

Alzheimer's disease (AD) is a progressive dementing illness in which the brain becomes littered with neuritic amyloid plaques. These plaques are associated with degenerating neuronal processes and consist primarily of fibrillar aggregates of the amyloid β peptide, Aβ. Aβ is derived from the amyloid protein precursor (APP), presumably via proteolytic cleavage of APP by β- and γ-secretases (1). The predominant forms of Aβ are 40 (Aβ40) or 42 (Aβ42) amino acids in length (2). Aβ42 and Aβ40 appear to be generated in different intracellular compartments, and Aβ42 has a greater propensity to self-aggregate into insoluble fibrils than Aβ40 (3, 4). Various point mutations in three distinct genes (APP, presenilin 1, presenilin 2) have been linked to autosomal dominant forms of familial AD (FAD). Notably, all of these mutations increase the production of Aβ42 (5).

Although Aβ has been shown to be neurotoxic in cell culture (6–8), a causal role for Aβ in widespread neuronal degeneration *in vivo* remains speculative. A particularly controversial question concerns whether Aβ-induced neurotoxicity requires deposition of aggregated Aβ into plaques (9–13). Transgenic mice in which full-length FAD-mutant APPs and Aβ are coexpressed at high levels develop typical neuritic amyloid plaques (14–17). However, loss of neurons so far has been identified in only one of these models (18) whereas two others showed no significant neuronal loss despite extensive cerebral Aβ deposition (19, 20). No electrophysiological studies have been reported in these models.

In the current study, we investigated in transgenic mice what early effects neuronal expression of full-length, FAD-mutant human APP has on the anatomy and physiology of the hippocampus, a central nervous system structure considered crucial for learning and memory. Our study demonstrates that the development of structural and functional neuronal deficits substantially precedes the formation of extracellular amyloid plaques and provides indirect evidence that Aβ, rather than APP itself, disrupts neuronal circuits in APP transgenic mice.

MATERIALS AND METHODS

Transgenic Mouse Lines. The platelet-derived growth factor (PDGF)–APP_{Ind} transgene (14, 21) and the generation of PDGF-APP_{Ind} line H6 (22) have been described. The Swedish mutation was introduced into the PDGF-APP_{Ind} transgene by PCR primer modification, and the correctness of PCR-amplified regions was confirmed by sequencing essentially as described (21). Microinjection of the PDGF-$APP_{Sw,\ Ind}$ transgene into (C57BL/6 × DBA/2) F2 one-cell embryos, identification of transgenic founders by slot blot analysis of genomic DNA, and selection of the $APP_{Sw,\ Ind}$ expresser line J9 by RNase protection assay (RPA) analysis were carried out according to previously described procedures (14, 21). Transgenic lines were maintained by crossing heterozygous transgenic mice with nontransgenic (C57BL/6 × DBA/2) F1 breeders. All transgenic mice were heterozygous with respect to the transgene. Nontransgenic littermates served as controls.

Mice were killed by decapitation under halothane anesthesia or by transcardial saline perfusion under anesthesia with chloral hydrate. Brains were removed rapidly and were dissected into regions to be snap-frozen immediately for later RNA and protein analyses, drop-fixed in phosphate-buffered 4% paraformaldehyde at 4°C for 24–72 h for neuropathological analysis, or used immediately for electrophysiological experiments.

RNA Analysis. RNA extractions and mRNA quantitations by solution hybridization RPA were performed as described (21) by using 10 μg of total RNA per sample in combination with the following ^{32}P-labeled antisense riboprobes [protected nucleotides (GenBank accession no.)]: human APP (hAPP) [nt2468–2657 (X06989) of hAPP fused via *Not*I linker with

The publication costs of this article were defrayed in part by page charge payment. This article must therefore be hereby marked "*advertisement*" in accordance with 18 U.S.C. §1734 solely to indicate this fact.

PNAS is available online at www.pnas.org.

Abbreviations: AD, Alzheimer's disease; APP, amyloid protein precursor; FAD, familial AD; PDGF, platelet-derived growth factor; RPA, RNase protection assay; FL, full-length; NMDA, *N*-methyl-D-aspartate; AMPA, α-amino-3-hydroxy-5-methyl-4-isoxazolepropionic acid; EPSC, excitatory postsynaptic current; hAPP, human APP; EPSP, excitatory postsynaptic potential; LTP, long-term potentiation; nt, nucleotides.

‡Present address: Centre National de la Recherche Scientifique, Institut Alfred Fessard, Avenue de la Terrasse, 91198 Gif-Yvette, France.

††To whom reprint requests should be addressed at: Gladstone Institute of Neurological Disease, P.O. Box 41900, San Francisco, CA 94141-9100. e-mail: Lmucke@gladstone.ucsf.edu.

nt2532–2656 (M24914) of SV40] and actin [nt480–559 (X03672) of mouse β-actin].

Detection of APP and Aβ. Homogenization of snap-frozen hippocampi in guanidine buffer and ELISA quantitations of human full-length (FL) and α-secreted (α) APP, total Aβ, and Aβ1–42 were performed as described (23). For detection of Aβ deposits, vibratome sections were incubated overnight at 4°C with biotinylated mouse monoclonal antibody 3D6 (diluted to 5 μg/ml), which specifically recognizes $A\beta_{1-5}$ (22, 23). Binding of primary antibody was detected with the Elite kit from Vector Laboratories by using diaminobenzidine and H_2O_2 for development. Sections were counterstained with 1% hematoxyline and were examined with a Vanox light microscope (Olympus, New Hyde Park, NY). Four sections were analyzed per mouse.

Assessment of Neurodegeneration. To determine the integrity of presynaptic terminals and neuronal cell bodies, vibratome sections were incubated overnight with mAbs against synaptophysin (1 μg/ml; Boehringer Ingelheim) or microtubule-associated protein 2 (1 μg/ml, Boehringer Ingelheim), followed by incubation with fluorescein isothiocyanate-conjugated horse anti-mouse IgG (1:75, Vector Laboratories). Sections then were transferred to SuperFrost slides (Fisher Scientific) and were mounted under glass coverslips with an antifading media (Vector Laboratories). The sections were imaged with a laser scanning confocal microscope (MRC1024; Bio-Rad) as described (14, 15) at a magnification of 630×. The three-dimensional numerical densities (expressed as counts per cubic millimeter) of synaptophysin-immunoreactive presynaptic terminals and microtubule-associated protein 2 immunoreactive neuronal cell bodies in the CA1 and CA3 subfields of the hippocampus were determined by using a modification of the stereological "disector" (24). A confocal image of synaptic boutons (disector grid: 105.26 μm^2) or neurons (disector grid: 2546.19 μm^2) was obtained, and then a second image was captured at the same x and y coordinates but at a greater depth (0.9 μm for synapses and 2 μm for neurons). The two images were superimposed, and the number of immunolabeled objects traversing both planes was counted. Twelve such disectors were spaced randomly through three serial hippocampal sections per mouse (avoiding overlap between disectors) and were analyzed. The mean counts obtained from 12 disectors per case were used for subsequent statistical analyses.

Electrophysiology. Hippocampal slice preparation and recording were performed as described (25). The artificial cerebrospinal fluid contained (in mM): 119 NaCl, 2.5 KCl, 2.5 $CaCl_2$, 1.3 Mg_2SO_4, 1.0 NaH_2PO_4, 26.2 $NaHCO_3$, and 10 glucose. Experiments were performed in the presence of picrotoxin (0.1 mM). Whole-cell recording electrodes were filled with a solution containing (in mM): 122.5 Cs-gluconate, 11 EGTA, 10 CsCl, 10 Hepes, 8 NaCl, 10 glucose, 1 $CaCl_2$, 4 Mg-ATP, and 0.3 Na_3-GTP. Unless otherwise specified, cells were voltage-clamped at −70 mV.

Basal synaptic transmission was assayed by determining input–output relations from extracellular field potential recordings in the stratum radiatum of CA1; the input was the peak amplitude of the fiber volley, and the output was the initial slope of the excitatory postsynaptic potential (EPSP). Long-term potentiation (LTP) was induced with four tetani delivered 20 s apart, each at 100 Hz for 1 s.

Paired-pulse facilitation was elicited by using an interstimulus interval of 40 ms. The *N*-methyl-D-aspartate (NMDA)/α-amino-3-hydroxy-5-methyl-4-isoxazolepropionic acid (AMPA) ratio was determined by holding cells at +50 mV. The peak amplitude of the average NMDA receptor-mediated excitatory postsynaptic current (EPSC) was divided by the peak amplitude of the average AMPA receptor-mediated EPSC recorded in the presence of the NMDA receptor antagonist D-2-amino-5-phosphonovaleric acid (D-APV) (50 μM), essentially as described (25).

In a separate series of experiments, we tested whether slice preparation itself could exacerbate excitotoxicity in transgenic slices and thereby lead to the observed deficits in basal synaptic transmission. Hippocampal slices were prepared from three 8- to 9-month-old APP_{Ind} mice either in the presence ($n = 11$) or absence ($n = 9$) of the glutamate receptor antagonist kynurenate (10 mM). Slopes of input–output relations were measured after removal of kynurenate. Pretreatment of slices with kynurenate did not prevent the impairment of input–output relations in transgenic slices ($P > 0.7$).

Statistical Analysis. For all experiments, mice and brain tissue samples were coded to blind investigators with respect to genotype. Unless indicated otherwise, data were expressed as mean ± SEM. Significance ($\alpha = 0.05$) was determined by Student's t test (pairwise comparisons), single-factor ANOVA followed by the Tukey-Kramer or Duncan's procedure (multiple comparisons), or the Pearson product–moment correlation coefficient t test (regression analyses).

RESULTS AND DISCUSSION

Age-Related Deposition of Aβ in Neuritic Plaques. In the first line of mice studied (H6) (22), the PDGF B chain promoter directs high-level neuronal expression of an alternatively spliced minigene encoding $717_{V\rightarrow F}$-mutant human APP695, APP751, and APP770 (21). Because the $717_{V\rightarrow F}$ substitution (APP770 numbering) has been linked to FAD in Indiana (26), hAPP carrying this mutation subsequently will be referred to as APP_{Ind}. High-level neuronal expression of the PDGF-APP_{Ind} fusion gene in another line of transgenic mice (line 109) has been shown to result in the development of AD-like neuropathology, including prominent amyloid plaques, dystrophic neurites, and gliosis (14, 15). Similar central nervous system alterations were subsequently also identified in transgenic models expressing FAD-mutant APPs from other promoters (16, 17).

Transgene expression levels in brains of APP_{Ind} mice from line H6 were similar to those of mice from line 109 (Fig. 1 *a* and *b*) (21, 23). Immunostaining with an hAPP-specific antibody (8E5) revealed widespread neuronal hAPP expression in brains of mice from line H6, with maximal levels found in the neocortex and hippocampus (data not shown). Hippocampal levels of hAPP and Aβ increased with age (Fig. 1*b*). In addition, deposition of Aβ in the form of AD-like amyloid plaques was age-dependent (Fig. 1 *c* and *d*): Amyloid plaques were found in 45% (9 of 20) of mice 8–10 months of age whereas no amyloid plaques were found in mice 2–5 months of age ($n = 9$). We therefore studied hippocampal anatomy and physiology of mice at both of these ages to see whether amyloid plaques are necessary for any observed neuronal deficits to occur.

Decreased Density of Presynaptic Terminals and Neurons Precedes Plaque Formation. Losses of the presynaptic vesicle protein synaptophysin in the prefrontal cortex (27) and hippocampus (28) have been shown to correlate with cognitive decline in human AD cases. In addition, there is loss of hippocampal neurons in AD with the most prominent losses seen in CA1 (29). The densities of synaptophysin-immunoreactive presynaptic terminals and microtubule-associated protein 2-positive neurons in the CA1 region were 26–32% lower in 2- to 3-month-old APP_{Ind} mice than in nontransgenic controls (Fig. 2). Neuronal loss in the CA3 region became statistically significant only in older animals but, in some of these cases, was rather striking (Fig. 2 *d* and *f*). These findings are in contrast to the lack of neuronal loss in mice from line 109 (ref. 20; E.M., unpublished observations), which express the same PDGF-APP_{Ind} construct. Strain differences may explain this discrepancy. Line 109 was maintained on an

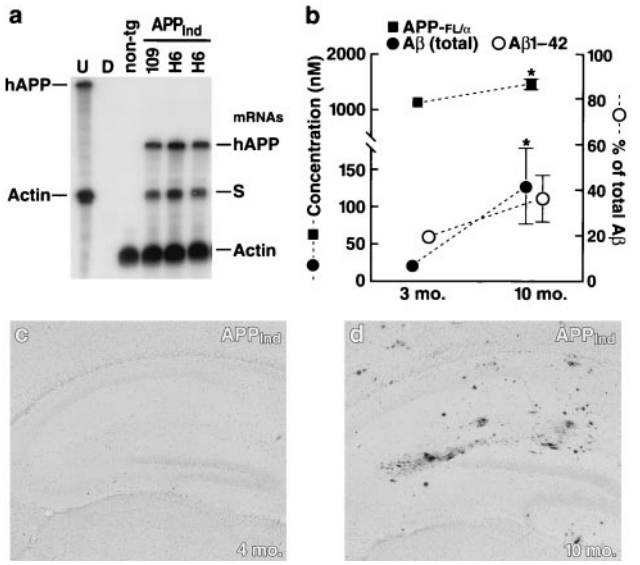

FIG. 1. Expression levels of transgene products and age-related Aβ deposition in brains of APP_{Ind} mice. (*a*) Representative autoradiograph showing comparable hAPP mRNA levels in brains of APP_{Ind} mice from line 109 and line H6. non-tg, nontransgenic control. Entire hemibrains were analyzed by RPA to determine steady-state mRNA levels. The leftmost lane shows signals of undigested (U) radiolabeled riboprobes (identified on left); the other lanes contained the same riboprobes plus either tRNA (D; no specific hybridization) or brain RNA samples, digested with RNases. Protected mRNAs are indicated on the right. The hAPP probe detects human but not mouse APP; it also recognizes a SV40 segment of transgene-derived mRNAs (labeled "S"). (*b*) Hippocampal levels of the following human antigens were quantitated by ELISAs in 3-month-old and in 10-month-old transgenic mice from line H6 (n = 7–8 per age group): full-length hAPP plus secreted hAPP cleaved at the α-secretase site (APP-FL/α), total Aβ, and Aβ1–42. ∗, $P < 0.05$. For several of the data points, the small error bars are hidden by the symbols. An additional 10-month-old transgenic mouse showed exceptionally high Aβ levels (APP-FL/α, 1,642 nM; total Aβ, 8,398 nM; Aβ1–42, 6824 nM); this outlier was excluded from the statistical analysis. (*c*) Hippocampus of a 4-month-old APP_{Ind} mouse (line H6). No Aβ deposits were detected by 3D6 immunostaining. (*d*) Hippocampus of a 10-month-old APP_{Ind} mouse (line H6) displaying multiple 3D6-positive Aβ deposits.

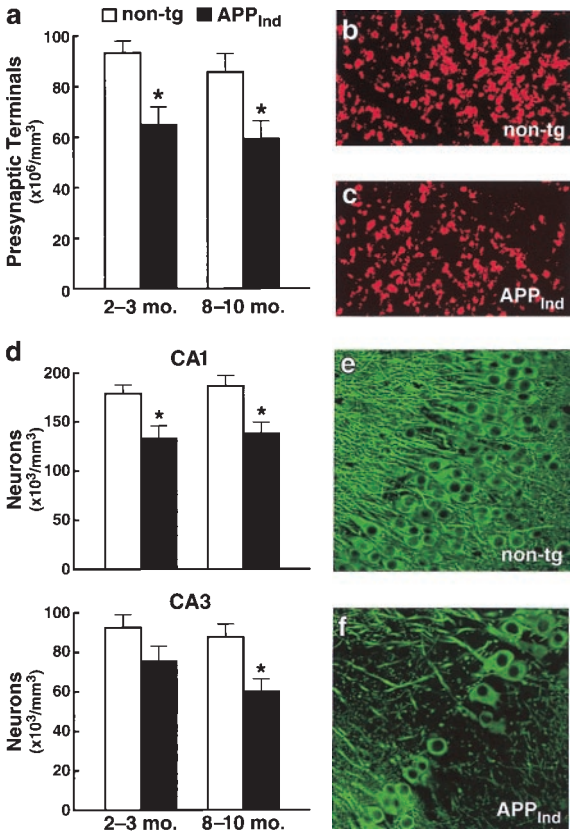

FIG. 2. Decreased density of presynaptic terminals and neurons in the hippocampus of APP_{Ind} mice (line H6). Vibratome sections of transgenic and nontransgenic brains were labeled with antibodies against a marker of presynaptic terminals (synaptophysin) (*a–c*) or a marker of neuronal cell bodies and dendrites (microtubule-associated protein 2) (*d–f*). (*a* and *d*) Quantitative assessment of presynaptic terminals in CA1 (*a*) and of neurons in CA1 and CA3 (*d*) (n = 9–11 mice per age range and genotype; ∗, $P < 0.05$ by Tukey-Kramer post hoc test compared with age-matched nontransgenic controls). (*b* and *c*) Representative confocal images of CA1 sections immunostained for synaptophysin. (*e* and *f*) Some 8- to 10-month-old transgenic mice showed a prominent loss of neurons in CA3 (*f*) that was unrelated to the presence or absence of amyloid plaques (data not shown). Such damage never was observed in age-matched nontransgenic littermate controls (*e*).

outbred background (C57BL/6 × DBA/2 × Swiss–Webster) whereas line H6 was maintained on a hybrid background (C57BL/6 × DBA/2). It is well known that susceptibility to other types of neuronal injury (e.g., excitotoxin-induced neurodegeneration) also can vary widely across mouse strains (30). Of interest, loss of neurons in CA1 has recently also been observed in another transgenic line in which high-level neuronal expression of FAD-mutant hAPP695 was directed by the Thy-1 promoter (18). To resolve the apparent discrepancies among different APP transgenic models will likely require concerted long-range efforts among different laboratories because all mouse lines will have to be backcrossed onto the same genetic background and analyzed side-by-side with the same methodologies.

Functional Decline Outstrips Neuropathological Alterations. Although histological identification of neuronal structures is informative, recent results caution against reliance on morphological information alone to make conclusions about the number of neuronal elements that are truly functional. Anatomical identification of presynaptic terminals can overestimate the number of functional synapses: presynaptically, there may not be active transmitter release (31–34), and postsynaptically, there may be an absence of receptors that are active at resting membrane potential (35, 36). Similarly, anatomical neuron counting may include neurons that are functionally removed from circuits (e.g., unable to generate action potentials). We therefore used electrophysiological techniques to assess whether there are functional changes in addition to the observed anatomical deficits, again at ages before and after amyloid plaque formation.

Extracellularly recorded EPSPs (field EPSPs) were used to assess the strength of basal synaptic transmission between hippocampal CA3 and CA1 cells. In 1- to 4-month-old APP_{Ind} mice, an ≈40% decrease in the slope of the input–output curve was observed (Fig. 3*a*), indicating a significant impairment in synaptic transmission. This functional deficit is similar in magnitude to that observed anatomically in young mice (Fig. 2*a*). However, by 8–10 months of age, a >80% deficit in basal synaptic transmission was observed (Fig. 3 *a* and *b*), suggesting a functional decline in great excess of morphological changes at that age.

The decrement in synaptic transmission is unlikely to be due to a decrease in the probability of transmitter release (p_r) because paired-pulse facilitation, which correlates inversely with the probability of transmitter release (37–39), remained unchanged (Fig. 3*c*). Nor can this decrement be explained by a graded decrease in the responsiveness to transmitter at individual synapses, because the average amplitude of miniature EPSCs was similar in transgenic mice and nontransgenic

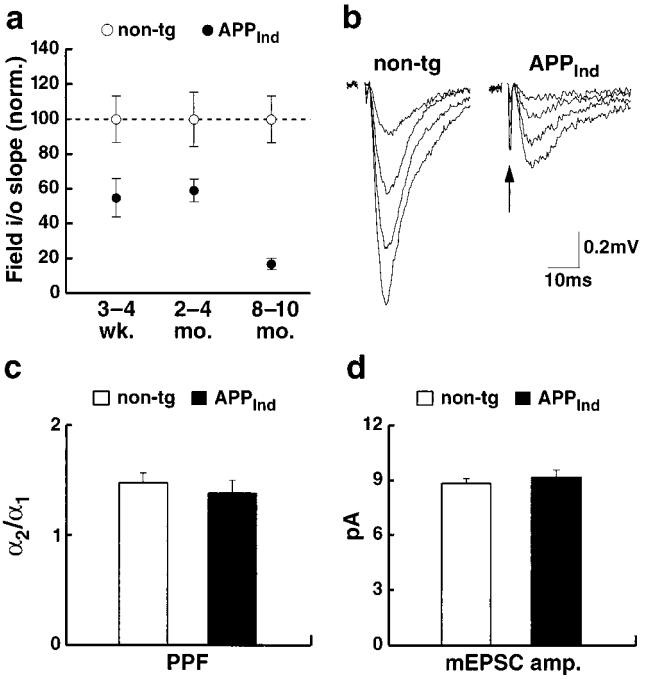

FIG. 3. Severe impairment in synaptic transmission between hippocampal CA3 and CA1 cells in APP_{Ind} mice (line H6). (*a*) The responsiveness of CA1 cells to increasing afferent fiber stimulation [slope of input–output (i/o) relation; see *Materials and Methods*] was determined in APP_{Ind} mice and nontransgenic controls to assess the strength of basal synaptic transmission. Each data point represents average results obtained in 17–87 slices obtained from 4–15 mice. For each age group, results were normalized to the mean value obtained in nontransgenic mice. Statistically significant differences were identified by Duncan's test between transgenic and nontransgenic mice ($P < 0.05$ at 3–4 weeks; $P < 0.01$ at 2–4 and 8–10 months) and between 2- to 4-month-old and 8- to 10-month-old transgenic mice ($P < 0.01$). (*b*) Representative field EPSPs at increasing stimulus strengths are shown for a nontransgenic and an APP_{Ind} mouse, illustrating that far higher stimulation strengths are required to elicit synaptic responses in APP_{Ind} mice. The fiber volley (arrow) is an indirect measure of the number of axons activated. (*c* and *d*) Paired-pulse facilitation (PPF) and quantal size were measured in CA1 cells of 8- to 10-month-old APP_{Ind} mice and nontransgenic controls. Each column represents average results from 6–8 hippocampal slices prepared from 2–4 mice. Paired-pulse facilitation was expressed as the ratio (α_2/α_1) of the average amplitudes of EPSCs evoked by a pair of closely spaced stimuli (*c*). Quantal size was determined as the mean amplitude of miniature EPSCs (mEPSCs) (*d*). pA, picoamps.

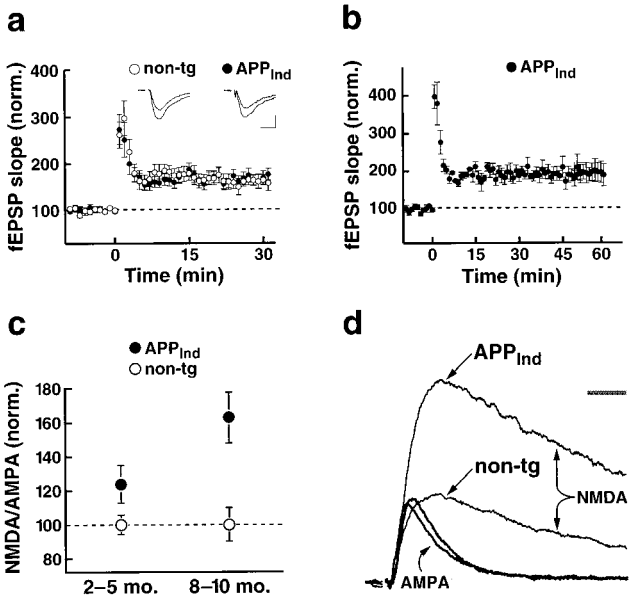

FIG. 4. APP_{Ind} mice (line H6) showed normal LTP and an increase in the NMDA/AMPA ratio in CA1 cells. (*a*) LTP was measured in 8- to 10-month-old APP_{Ind} mice (9 slices from 5 mice) and nontransgenic controls (7 slices from 3 mice) at 30 min after induction. Insets show average EPSPs at 5 min before and 50 min after LTP induction in representative experiments from an 8-month-old APP_{Ind} mouse and an age-matched nontransgenic control. Scale: 0.2 mV (nontransgenic), 0.1 mV (APP_{Ind}); 10 ms. fEPSP = field EPSP. (*b*) In a subset of these APP_{Ind} mice ($n = 3$), LTP was monitored until 1 h after induction. (*c*) The ratio of amplitudes of NMDA receptor-mediated to AMPA receptor-mediated EPSCs in individual CA1 cells was determined. For each age group, results were normalized to the mean value obtained in nontransgenic mice. Each data point represents data from 12–27 slices from 3–9 mice. At all ages analyzed, APP_{Ind} mice showed an increase in the mean NMDA/AMPA ratio compared with nontransgenic controls ($P < 0.01$). There was an age-related increase in NMDA/AMPA ratios in transgenic ($P < 0.01$) but not in nontransgenic mice. *P* values were determined by Duncan's test. (*d*) Example EPSCs recorded in two representative CA1 cells from a 9-month-old APP_{Ind} mouse and an age-matched nontransgenic control. EPSCs were scaled such that the AMPA receptor-mediated EPSCs from each cell are of equal amplitude. (Bar = 20 ms.)

controls (Fig. 3*d*). Because neither the reliability nor the strength of individual synapses decreased, it is likely that a significant decrease in the number of functional synapses occurs between 3 and 8 months of age. This change is unlikely to be caused by the extracellular deposition of amyloid plaques because the magnitude of the functional deficit in 8- to 10-month-old APP_{Ind} mice did not correlate with the presence of plaques ($P > 0.5$, $n = 6$ mice; data not shown).

Analysis of Remaining Functional Synapses. Expression of APP_{Ind} thus appears to disconnect, both anatomically and functionally, neuronal subregions in the hippocampus. We next asked whether, among the functional synapses that remain, there are any alterations in the ability to undergo plastic change. We therefore measured LTP in the CA1 region of APP_{Ind} mice but found no impairment (Fig. 4 *a* and *b*). At 30 min after induction, LTP was 167 ± 13% in APP_{Ind} mice ($n = 9$) and 163 ± 13% in nontransgenic controls ($n = 7$) ($P > 0.8$; age, 8–10 months). To ensure that the LTP in these mice was stable, in a subset of experiments LTP was monitored until 1 h after induction (Fig. 4*b*); it averaged 199 ± 27% in 8-month-old APP_{Ind} mice ($n = 3$). In contrast, an impairment of LTP previously has been reported in transgenic mice in which a C-terminal fragment of hAPP was expressed (40), presumably in the cytoplasmic compartment of neurons, as opposed to the transmembrane localization of endogenous hAPP. The handling, trafficking, and signaling properties of this hAPP fragment are likely different from those of the full-length hAPP molecule and its natural cleavage products, which may explain the different results obtained in the two mouse models.

Another potential change at individual synapses is the proportion of synaptic transmission mediated by different receptor subtypes (41–44). The EPSC has two components generated by the NMDA and AMPA subtypes of glutamate receptors. We observed in APP_{Ind} mice an increased ratio of the NMDA versus AMPA components of the EPSC (Fig. 4 *c* and *d*), suggesting either an up-regulation of NMDA receptors or the inhibition/internalization of AMPA receptors at individual synapses. Because the AMPA receptor component of the miniature EPSCs did not decrease in amplitude in APP_{Ind} mice (Fig. 3*d*), an up-regulation of NMDA receptors is more likely. Consistent with this interpretation, acute application of recombinant Aβ has been reported to selectively up-regulate NMDA receptor-mediated, but not AMPA receptor-mediated, synaptic transmission in hippocampal slices (45). Conceivably, Aβ-induced up-regulation of NMDA receptors

could contribute to excitotoxicity and neuronal degeneration (46).

Increasing Aβ Production While Decreasing hAPP Expression Worsens Neuronal Deficits. In all AD models in which Aβ is expressed from the full-length precursor molecule, overexpression of Aβ is inseparably linked to overexpression of APP itself. Because APP could affect neuronal function through a number of different mechanisms (47–52), it is important to determine whether APP *per se* might be responsible for functional deficits observed in these models. We therefore generated a second mouse line in which Aβ is expressed at high levels in the context of relatively low levels of hAPP expression. This second mouse line ($APP_{Sw,\ Ind}$ line J9) was generated by introducing into the original APP_{Ind} transgene the "Swedish" mutation ($670_{K\rightarrow N}/671_{M\rightarrow L}$) (53), which has been shown to increase the generation of Aβ (54, 55). Mice from $APP_{Sw,\ Ind}$ line J9 had almost twice as much Aβ in their hippocampi as mice from APP_{Ind} line H6 but much lower hAPP levels (Fig. 5 *a–c*).

Because they are sensitive to both functional and anatomical changes, electrophysiological measures were used to compare 2- to 4-month-old mice from lines H6 and J9. We reasoned that, if APP itself exerted the predominant deleterious effect in these models, mice from line J9 should display smaller deficits than mice from line H6 whereas the opposite would occur if Aβ were the main culprit. As shown in Fig. 5*d*, the deficit in synaptic transmission in line J9 was almost twice as large as that in line H6. These findings are consistent with an insidious role for Aβ; however, to determine whether the neuronal deficits in these models are caused solely by Aβ, it will be necessary to develop compounds that selectively block Aβ production or activity without affecting other APP metabolites.

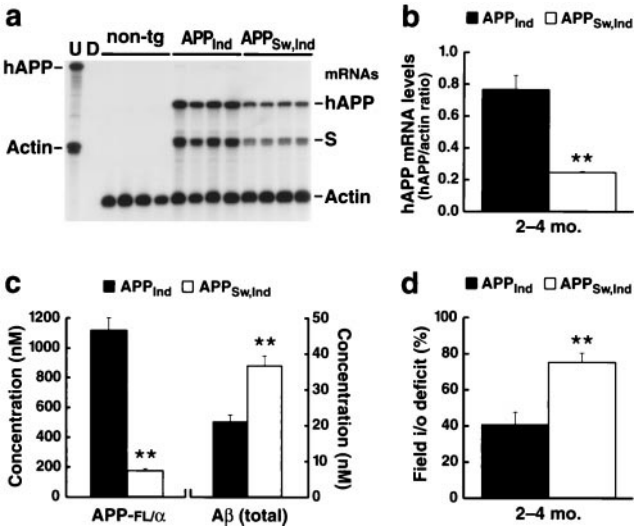

FIG. 5. Increased Aβ levels exacerbate synaptic transmission deficits in the context of lower APP expression. (*a*) Autoradiograph depicting an RPA analysis of cerebral hAPP levels in APP_{Ind} (line H6) and $APP_{Sw,\ Ind}$ (line J9) mice ($n = 4$ mice/line; age, 2–4 months). The APP probe used detects human but not mouse APP; it also recognizes an SV40 segment of transgene-derived mRNAs (S). Conventions otherwise as in Fig. 1*a*. (*b*) The signals shown in *a* were quantified by phosphorimager analysis and were expressed as hAPP to actin ratios to correct for variations in RNA content/loading. **, $P < 0.01$. (*c*) Hippocampal levels of human APP-FL/α and total Aβ were determined by ELISAs in APP_{Ind} (line H6) and $APP_{Sw,\ Ind}$ (line J9) mice ($n = 8$ mice/line; age, 2–4 months). **, $P < 0.001$. Note that the hAPP-FL/α ELISA does not detect β-secreted hAPP. This may explain why hAPP expression levels in $APP_{Sw,\ Ind}$ mice were lower by ELISA than by RPA analysis. (*d*) Comparison of deficits in field input–output relations in 2- to 4-month-old APP_{Ind} (line H6) and $APP_{Sw,\ Ind}$ (line J9) mice. For each line, results were expressed as the percent deficit relative to the mean value obtained in nontransgenic controls. The APP_{Ind} analysis shown here was based on the same raw data as the analysis of 2- to 4-month-old APP_{Ind} mice included in Fig. 3*a*. These data were compared with results obtained in 18 slices prepared from three age-matched $APP_{Sw,\ Ind}$ mice.

Although amyloid plaques were found in $APP_{Sw,\ Ind}$ mice from line J9 at 8–10 months of age, no amyloid plaques were detected in these mice at ages analyzed electrophysiologically (0 of 19 mice at 2–4 months of age). This finding underscores the fact that extracellular deposition of fibrillar Aβ is not required for the development of severe functional deficits in these models. If not extracellular deposits of fibrillar Aβ, what, then, is causing these impairments? Possibilities include neurotoxic effects induced by diffusible Aβ oligomers (8) or by intraneuronal accumulation of Aβ (4, 15, 56).

It is tempting to speculate that the disruption of neuronal connectivity we identified in the hippocampus of APP mice may relate to cognitive impairments seen in humans with AD. Although great caution must be applied when extrapolating from findings obtained in experimental models to complex human diseases, our results could provide a circuit-level explanation for the discrepancies observed between plaque load and functional deficits in humans with AD (11–13). They also suggest that inhibition of plaque formation alone may not prevent Aβ neurotoxicity *in vivo* and that inhibition of neuronal Aβ production may be required to achieve this therapeutic goal.

We thank M. Frerking for helpful comments on the manuscript, D. Selig for computer software allowing online data acquisition, and G. Costa for administrative assistance. This work was supported by grants from the National Institutes of Health to L.M., E.M., R.C.M., and R.A.N., the Human Frontiers Science Program to R.C.M., the McKnight Endowment Fund for Neuroscience to R.C.M., and the Office of Naval Research to A.Y.H.

1. Checler, F. (1995) *J. Neurochem.* **65,** 1431–1444.
2. Wang, R., Sweeney, D., Gandy, S. E. & Sisodia, S. S. (1996) *J. Biol. Chem.* **271,** 31894–31902.
3. Harper, J. D. & Lansbury, P. T., Jr. (1997) *Annu. Rev. Biochem.* **66,** 385–407.
4. Lee, S. J., Liyanage, U., Bickel, P. E., Xia, W. M., Lansbury, P. T., Jr. & Kosik, K. S. (1998) *Nat. Med.* **4,** 730–734.
5. Lendon, C. L., Ashall, F. & Goate, A. M. (1997) *J. Am. Med. Assoc.* **277,** 825–831.
6. Yankner, B. A., Duffy, L. K. & Kirschner, D. A. (1990) *Science* **250,** 279–282.
7. Pike, C. J., Burdick, D., Walencewicz, A. J., Glabe, C. G. & Cotman, C. W. (1993) *J. Neurosci.* **13,** 1676–1687.
8. Lambert, M. P., Barlow, A. K., Chromy, B. A., Edwards, C., Freed, R., Liosatos, M., Morgan, T. E., Rozovsky, I., Trommer, B., Viola, K. L., *et al.* (1998) *Proc. Natl. Acad. Sci. USA* **95,** 6448–6453.
9. Cummings, B. J., Pike, C. J., Shankle, R. & Cotman, C. W. (1996) *Neurobiol. Aging* **17,** 921–933.
10. Bartoo, G. T., Nochlin, D., Chang, D., Kim, Y. & Sumi, S. M. (1997) *J. Neuropathol. Exp. Neurol.* **56,** 531–540.
11. Terry, R. D. (1996) *J. Neuropathol. Exp. Neurol.* **55,** 1023–1025.
12. Davis, J. N. & Chisholm, J. C. (1997) *Trends Neurosci.* **20,** 558–559.
13. Gomez-Isla, T., Hollister, R., West, H., Mui, S., Growdon, J. H., Petersen, R. C., Parisi, J. E. & Hyman, B. T. (1997) *Ann. Neurol.* **41,** 17–24.
14. Games, D., Adams, D., Alessandrini, R., Barbour, R., Berthelette, P., Blackwell, C., Carr, T., Clemens, J., Donaldson, T., Gillespie, F., *et al.* (1995) *Nature (London)* **373,** 523–527.
15. Masliah, E., Sisk, A., Mallory, M., Mucke, L., Schenk, D. & Games, D. (1996) *J. Neurosci.* **16,** 5795–5811.
16. Hsiao, K., Chapman, P., Nilsen, S., Eckman, C., Harigaya, Y., Younkin, S., Yang, F. S. & Cole, G. (1996) *Science* **274,** 99–102.
17. Sturchler-Pierrat, C., Abramowski, D., Duke, M., Wiederhold, K. H., Mistl, C., Rothacher, S., Ledermann, B., Burki, K., Frey, P., Paganetti, P. A., *et al.* (1997) *Proc. Natl. Acad. Sci. USA* **94,** 13287–13292.

18. Calhoun, M. E., Wiederhold, K. H., Abramowski, D., Phinney, A. L., Probst, A., Sturchler-Pierrat, C., Staufenbiel, M., Sommer, B. & Jucker, M. (1998) *Nature (London)* **395,** 755–756.
19. Irizarry, M. C., McNamara, M., Fedorchak, K., Hsiao, K. & Hyman, B. T. (1997) *J. Neuropathol. Exp. Neurol.* **56,** 965–973.
20. Irizarry, M. C., Soriano, F., McNamara, M., Page, K. J., Schenk, D., Games, D. & Hyman, B. T. (1997) *J. Neurosci.* **17,** 7053–7059.
21. Rockenstein, E. M., McConlogue, L., Tan, H., Gordon, M., Power, M., Masliah, E. & Mucke, L. (1995) *J. Biol. Chem.* **270,** 28257–28267.
22. Wyss-Coray, T., Masliah, E., Mallory, M., McConlogue, L., Johnson-Wood, K., Lin, C. & Mucke, L. (1997) *Nature (London)* **389,** 603–606.
23. Johnson-Wood, K., Lee, M., Motter, R., Hu, K., Gordon, G., Barbour, R., Khan, K., Gordon, M., Tan, H., Games, D. *et al.* (1997) *Proc. Natl. Acad. Sci. USA* **94,** 1550–1555.
24. Everall, I. P., DeTeresa, R., Terry, R. & Masliah, E. (1997) *J. Neuropathol. Exp. Neurol.* **56,** 1202–1206.
25. Hsia, A., Malenka, R. & Nicoll, R. (1998) *J. Neurophysiol.* **79,** 2013–2024.
26. Murrell, J., Farlow, M., Ghetti, B. & Benson, M. D. (1991) *Science* **254,** 97–99.
27. Terry, R. D., Masliah, E., Salmon, D. P., Butters, N., DeTeresa, R., Hill, R., Hansen, L. A. & Katzman, R. (1991) *Ann. Neurol.* **30,** 572–580.
28. Sze, C.-I., Troncoso, J. C., Kawas, C., Mouton, P., Price, D. L. & Martin, L. J. (1997) *J. Neuropathol. Exp. Neurol.* **56,** 933–944.
29. West, M. & Gundersen, H. (1990) *J. Comp. Neurol.* **296,** 1–22.
30. Schauwecker, P. E. & Steward, O. (1997) *Proc. Natl. Acad. Sci. USA* **94,** 4103–4108.
31. Redman, S. (1990) *Physiol. Rev.* **70,** 165–198.
32. Faber, D. S., Lin, J. W. & Korn, H. (1991) *Ann. N.Y. Acad. Sci.* **627,** 151–164.
33. Wojtowicz, J. M., Smith, B. R. & Atwood, H. L. (1991) *Ann. N.Y. Acad. Sci.* **627,** 169–179.
34. Tong, G., Malenka, R. C. & Nicoll, R. A. (1996) *Neuron* **16,** 1147–1157.
35. Isaac, J. T., Nicoll, R. A. & Malenka, R. C. (1995) *Neuron* **15,** 427–434.
36. Liao, D., Hessler, N. A. & Malinow, R. (1995) *Nature (London)* **375,** 400–404.
37. Zucker, R. (1989) *Annu. Rev. Neurosci.* **12,** 13–31.
38. Manabe, T., Wyllie, D., Perkel, D. & Nicoll, R. (1993) *J. Neurophysiol.* **70,** 1451–1459.
39. Dobrunz, L. & Stevens, C. (1997) *Neuron* **14,** 995–1008.
40. Nalbantoglu, J., Tirado-Santiago, G., Lahsaini, A., Poirier, J., Goncalves, O., Verge, G., Momoli, F., Welner, S. A., Massicotte, G., Julien, J. P., *et al.* (1997) *Nature (London)* **387,** 500–505.
41. Ben-Ari, Y., Khazipov, R., Leinekugel, X., Caillard, O. & Gaiarsa, J. L. (1997) *Trends Neurosci.* **20,** 523–529.
42. Turrigiano, G. G., Leslie, K. R., Desai, N. S., Rutherford, L. C. & Nelson, S. B. (1998) *Nature (London)* **391,** 892–896.
43. Lissin, D. V., Gomperts, S. N., Carroll, R. C., Christine, C. W., Kalman, D., Kitamura, M., Hardy, S., Nicoll, R. A., Malenka, R. C. & von Zastrow, M. (1998) *Proc. Natl. Acad. Sci. USA* **95,** 7097–7102.
44. Malenka, R. C. & Nicoll, R. A. (1997) *Neuron* **19,** 473–476.
45. Wu, J. Q., Anwyl, R. & Rowan, M. J. (1995) *NeuroReport* **6,** 2409–2413.
46. Lipton, S. A. & Rosenberg, P. A. (1994) *N. Engl. J. Med.* **330,** 613–622.
47. Milward, E. A., Papadopoulos, R., Fuller, S. J., Moir, R. D., Small, D., Beyreuther, K. & Masters, C. L. (1992) *Neuron* **9,** 129–137.
48. Mattson, M. P., Cheng, B., Culwell, A. R., Esch, F. S., Lieberburg, I. & Rydel, R. E. (1993) *Neuron* **10,** 243–254.
49. Greenberg, S. M., Koo, E. H., Selkoe, D. J., Qiu, W. Q. & Kosik, K. S. (1994) *Proc. Natl. Acad. Sci. USA* **91,** 7104–7108.
50. Multhaup, G., Schlicksupp, A., Hesse, L., Beher, D., Ruppert, T., Masters, C. L. & Beyreuther, K. (1996) *Science* **271,** 1406–1409.
51. Okamoto, T., Takeda, S., Giambarella, U., Murayama, Y., Matsui, T., Katada, T., Matsuura, Y. & Nishimoto, I. (1996) *EMBO J.* **15,** 3769–3777.
52. Masliah, E., Raber, J., Alford, M., Mallory, M., Mattson, M. P., Yang, D., Wong, D. & Mucke, L. (1998) *J. Biol. Chem.* **273,** 12548–12554.
53. Mullan, M., Crawford, F., Axelman, K., Houlden, H., Lilius, L., Winblad, B. & Lannfelt, L. (1992) *Nat. Genet.* **1,** 345–347.
54. Citron, M., Oltersdorf, T., Haass, C., McConlogue, L., Hung, A. Y., Seubert, P., Vigo-Pelfrey, C., Lieberburg, I. & Selkoe, D. J. (1992) *Nature (London)* **360,** 672–674.
55. Younkin, S. G. (1995) *Ann. Neurol.* **37,** 287–288.
56. Turner, R. S., Suzuki, N., Chyung, A. S. C., Younkin, S. G. & Lee, V. M.-Y. (1996) *J. Biol. Chem.* **271,** 8966–8970.